arXiv:hep-ph/0009158v1 13 Sep 2000

University of Wisconsin - Madison

MADPH-00-1191
IFT–P.076/2000
September 2000

Observing an invisible Higgs boson

O. J. P. Éboli[1] and D. Zeppenfeld[2]
[1]*Instituto de Física Teórica – UNESP*
R. Pamplona 145, 01405-900 São Paulo, Brazil
[2]*Department of Physics, University of Wisconsin, Madison, WI 53706, USA*

Abstract

Given its weak coupling to bottom quarks and tau leptons, the Higgs boson may predominantly decay into invisible particles like gravitinos, neutralinos, or gravitons. We consider the manifestation of such an invisibly decaying Higgs boson in weak boson fusion at the CERN LHC. Distinctive kinematic distributions of the two quark jets of the signal as compared to Zjj and Wjj backgrounds allow to restrict the Higgs branching ratio to 'invisible' final states to some 13% with 10 fb^{-1} of data, provided events with two energetic forward jets of high dijet invariant mass and with substantial missing transverse momentum can be triggered efficiently. It is also possible to discover these particles with masses up to 480 GeV in weak boson fusion, at the 5σ level, provided their invisible branching ratio is close to 100%.

I. INTRODUCTION

Some extensions of the Standard Model (SM) exhibit Higgs bosons which can decay into stable neutral weakly interacting particles, therefore giving rise to invisible final states. In supersymmetric models the Higgs bosons can decay with a large branching ratio into lightest neutralinos or gravitinos in some region of the parameter space [1], leading to an invisible final state if R parity is conserved. Invisible Higgs decays also happen in models with an enlarged symmetry breaking sector, *e.g.* in Majoron models [2,3], where the Higgs disintegrates into light weakly interacting scalars. In the scenario of large extra dimensions, proposed by Arkani-Hamed, Dimopoulos and Dvali [4], it is possible that the Higgs boson mixes with scalar fields arising from gravity propagating in extra dimensions [5]. This mixing can lead to a sizeable invisible width for the Higgs.

Certainly the presence of invisible decays modifies considerably the Higgs boson searches, making it much more difficult. At e^+e^- colliders the problem is not very severe, and it has been shown that the Higgs parameter space can be probed completely [6]. Presently, the LEP II collaborations exclude invisible Higgs masses up to 106.7 GeV [7]. On the other hand, the Higgs search at hadron colliders is much more difficult in the presence of such invisible decays. Previous studies have analyzed ZH and WH associated production [8] and $t\bar{t}H$ production [9] as promising channels. Considering statistical errors only and assuming that the Higgs couplings are the SM ones and that the invisible branching ratio effectively is 100%, the associated ZH production was estimated to be sensitive to Higgs masses $m_H \lesssim 150$ GeV [8] at the CERN LHC while $t\bar{t}H$ production might extend the Higgs mass range to 250 GeV [9]. Both searches must deal with signal cross sections in the few fb range or below, however, and detector resolution and background normalization errors become crucial because signal and background distributions have virtually identical shapes after cuts.

In this work we show that the LHC's potential to unravel the existence of invisibly decaying Higgs bosons can be considerably extended by studying Higgs production via weak boson fusion. Weak boson fusion (WBF) is a copious source of Higgs bosons at the LHC, yielding signal cross sections, after cuts, of order 100 fb, as we shall see. Furthermore, the presence of very energetic forward jets in the signal, with characteristic azimuthal angle correlations, allows us to tag the Higgs events and to efficiently suppress the backgrounds. It has been shown that WBF is among the most promising search channels in the 120–200 GeV Higgs mass range. It is possible to observe an intermediate mass Higgs boson through its decays $H \to \gamma\gamma$ [10], $H \to W^*W^* \to e^\pm\mu^\mp \not{p}_T$ [11], and even $H \to \tau^+\tau^-$ [12]. Here we extend this list to include otherwise invisible decay modes.

This paper is organized as follows. In Section II, we describe the techniques used to evaluate the relevant cross sections, while Section III contains the main characteristics of the signal and backgrounds and the cuts chosen to enhance the invisible Higgs signal. In Section IV, we present a detailed discussion of how to use data to predict the exact background normalization. Our results and conclusions are presented in Section V.

II. CALCULATIONAL TOOLS

We are considering the production of Higgs bosons in WBF, $qq \to qqVV \to qqH$ ($V = W$ or Z), with subsequent decay to undetectable particles. The signal is thus characterized by two

quark jets, which typically enter in the forward and backward regions of the detector and are widely separated in pseudorapidity, and by a large transverse momentum imbalance, due to the Higgs' invisible decay products. Significant backgrounds can arise from any processes leading to two jets and missing transverse momentum, such as Zjj production with subsequent decay $Z \to \bar{\nu}\nu$ or Wjj production with $W \to \ell\nu$ decay where the charged lepton is not identified. Another source are QCD dijet and multijet events with large missing transverse momentum generated by energy mismeasurements or from high p_T particles escaping through the beam-hole. These purely QCD processes possess a potentially very large cross section. In mismeasured two jet events, the missing p_T points in the direction of the jets and we use this fact to suppress this background. However, this is not true for the production of 3 or more jets and we include this QCD jjj background in our analysis.

The signal and backgrounds are simulated at the parton level with full tree level matrix elements. This was accomplished by numerically evaluating helicity amplitudes for all subprocesses. Backgrounds include all order α_s^2 real emission corrections to Drell-Yan production (to be called QCD Wjj and Zjj processes) and cross sections are calculated with code based on Ref. [13]. The second large class of processes are the signal and the electroweak background, EW Wjj and Zjj production, with contributions from the t-channel exchange of an electroweak boson off which the final state W, Z or Higgs is radiated. The code for these processes is based on Ref. [14], and was checked with matrix elements generated using the package Madgraph [15]. Madgraph code was also used to simulate the QCD jjj background at tree level. For all QCD effects, the running of the strong coupling constant is evaluated at one-loop order, with $\alpha_s(M_Z) = 0.12$. We employed CTEQ4L parton distribution functions [16] throughout. The factorization scale was chosen as $\mu_f = \min(p_T)$ of the defined jets. We took the electroweak parameters $\sin^2\theta_W = 0.23124$, $\alpha_{em} = 1/128.93$, $m_Z = 91.189$ GeV, and $m_W = 79.95$ GeV, which was obtained imposing the tree level relation $\cos\theta_W = m_W/m_Z$. For the QCD jjj background, for which detector effects produce the missing p_T, we simulate experimental resolutions by smearing the energies (but not directions) of all final state partons with a Gaussian error given by $\Delta(E)/E = 0.5/\sqrt{E} \oplus 0.02$ (E in GeV).

$W \to l\nu$ decays in Wjj events lead to a $jj\not{p}_T$ signature when the charged lepton $l = e, \mu, \tau$ is not identified. A precise modeling of this background requires a full detector simulation. We estimate the Wjj backgrounds by assuming that in the central region, $|\eta_l| < 2.5$, all muons, electrons and taus with $p_T(l) > 5, 10, 20$ GeV, respectively, can be vetoed, while any charged leptons below these thresholds will be misidentified and counted in the p_T balance only. In the forward regions, $2.5 < |\eta_l| < 5$, a lepton veto is taken to be impossible. Here, muons are assumed to give no p_T deposit in the calorimeters, in contrast to electrons and taus whose entire energy is recorded. Note that the resulting Wjj background, within jet cuts given below, is about half the event rate of all $Wjj, W \to l\nu$ events with $p_T(\nu) > 100$ GeV, i.e. we are certain not to seriously underestimate the Wjj background.

An important feature of the WBF signal is the absence of color exchange between the final state quarks, which leads to a depletion of gluon emission in the region between the two tagging jets. We can enhance the signal to background ratio by vetoing additional soft jet activity in the central region [17]. A central jet veto is ineffective against the EW Wjj and Zjj backgrounds which possess the same color structure as the signal. For the QCD backgrounds, however, there is color exchange in the t-channel and consequently a more abundant production of soft jets, with $p_T > 20$ GeV, in the central region [14]. The probability of an

event to survive such a central jet veto has been analyzed for various processes in Ref. [18], from which we take the veto survival probabilities of Table I which are appropriate for the hard tagging jet cuts to be used below.

The cross section for Higgs boson production via WBF is well known within the framework of the SM. We should keep in mind that this production cross section might be diluted in extensions of the SM. For instance, it is suppressed by factors $\sin^2(\beta-\alpha)$ or $\cos^2(\beta-\alpha)$ in supersymmetric models. Any suppression in the production cross section has the same effect, for our study, as a branching ratio of invisible Higgs decays below unity, and we will not separate these effects in the following.

III. SIGNAL AND BACKGROUND PROPERTIES

The main features of the production of an invisible Higgs boson via WBF are the presence of two very energetic forward jets as well as a large missing transverse momentum. Therefore, we initially impose the following jet tagging cuts and missing momentum cut

$$p_T^j > 40 \text{ GeV} \quad , \quad |\eta_j| < 5.0$$
$$|\eta_{j1} - \eta_{j2}| > 4.4 \quad , \quad \eta_{j1} \cdot \eta_{j2} < 0 \ , \tag{1}$$
$$\not{p}_T > 100 \text{ GeV} \ . \tag{2}$$

A further reduction of the backgrounds, with good signal efficiency, is achieved by requiring a large invariant mass, M_{jj}, of the two tagging jets,

$$M_{jj} > 1200 \text{ GeV} \ , \tag{3}$$

and by selecting events where the azimuthal angle between the tagging jets, ϕ_{jj} (measured in radians) is relatively small,

$$\phi_{jj} < 1 \ , \tag{4}$$

In order to motivate our choice of the $\not{p}_T$ cut, we display, in Fig. 1, the $\not{p}_T$ spectrum after the cuts (1) and (3), but without a central jet veto. The signal exhibits a peak around $\not{p}_T \simeq 100$ GeV and it is much smaller than the backgrounds at small $\not{p}_T$. Missing p_T generated by the QCD jjj background falls rapidly and this background becomes negligible above $\not{p}_T = 100$ GeV. Note that we require $\phi_{jj} < 2.6$ for the two tagging jets of the QCD jjj background, in order to avoid the soft singularities present near $\phi_{jj} = \pi$. Well above $\not{p}_T \simeq 100$ GeV, the missing p_T spectra of the signal and the Zjj backgrounds have the same slope. Hence, a tightening of the $\not{p}_T$ cut soon becomes useless.

The QCD backgrounds involve initial and final state gluons which tend to be softer than the quarks in WBF. In Fig. 2, this is reflected by the steeper falloff of the QCD backgrounds as M_{jj}, the dijet invariant mass, is increased. The $M_{jj} > 1200$ GeV requirement reduces these backgrounds sufficiently. Note that no central jet veto is included in Fig. 2. A further improvement of the signal to background ratio is possible by tightening the M_{jj} cut, but this will not be pursued in the following.

The most distinct remaining difference between the Higgs signal and all backgrounds is the azimuthal angle correlation of the two tagging jets. The ϕ_{jj} distributions within the cuts

(1-3) and including the central jet veto efficiencies of Table I are shown in Fig. 3. The $hV_\mu V^\mu$ coupling of the Higgs boson in WBF favors Higgs emission opposite to both tagging jets, which leads to small values of ϕ_{jj}. The Wjj and Zjj backgrounds, on the other hand, are smallest in this region and prefer back to back jets. The distinct shape difference of the ϕ_{jj} distributions provides very powerful tools to probe for a Higgs contribution, either by a full shape analysis or by the $\phi_{jj} < 1$ cut of (4).

The effect of such a cut is presented in Tables II and III, where background and signal cross sections are given after imposing the cuts (1-3) and (1-4). With an integrated luminosity of 10 fb^{-1} a total of 1670 background and of order 400 to 1000 signal events with $\phi_{jj} < 1$ are expected for an invisible branching fraction Br$(H \to \text{invisible}) = 1$, giving a highly significant signal when statistical errors only are considered.

IV. PREDICTING THE BACKGROUND

Finding, or constraining, an invisibly decaying Higgs boson signal in $jj\not{p}_T$ events is essentially a counting experiment since a resonance in the invariant mass distribution of the Higgs decay products cannot be extracted. The sensitivity of the search is thus determined by the precision with which the background rate in the search region can be predicted. Since the signal selection is demanding, including double forward jet tagging and central jet vetoing techniques whose acceptance cannot be calculated with sufficient precision in perturbative QCD, the background levels need to be determined directly from LHC data.

Fortunately, a sizable sample of Vjj events ($V = W$ or Z), with fully identified charged leptons from the V decay, will be available within the hadronic acceptance cuts discussed above. For Zjj events with two identified charged leptons, the $\not{p}_T > 100$ GeV cut is equivalent to $p_T(Z) > 100$ GeV and the only difference to the $Zjj,\ Z \to \nu\bar{\nu}$ background is due to minimal charged lepton p_T and rapidity cuts which are needed to insure their observability. The cross section for QCD and EW $Zjj,\ Z \to l^+l^-$ events ($l = e,\ \mu$), with $p_T(l) > 15$ GeV, $|\eta_l| < 2.5$ and within the cuts (1-3), including the central jet veto probabilities of Table I, is about 87 fb, of which 16.6 fb are expected in the $\phi_{jj} < 1$ region. Thus an effective luminosity of 10 fb^{-1} is sufficient to measure the Zjj background in the two regions $\phi_{jj} > 1$ and $\phi_{jj} < 1$ with relative errors of 3.8% and 7.8%, respectively.

The level of the Wjj background can be extracted from $W^\pm \to l^\pm\nu$ events, with hadronic cuts as given above and the additional requirements $p_T(W) > 100$ GeV and $p_T(l) > 25$ GeV, $|\eta_l| < 2.5$. The combined cross section for QCD and EW $(W \to l\nu)jj$ events, including central jet veto, is 184 fb (975 fb) with (without) the $\phi_{jj} < 1$ requirement. With an effective luminosity of 10 fb^{-1} this translates into a statistical error of a mere 2.3% for the prediction of the total Wjj background within the cuts (1-4). Central jet veto efficiencies will be almost identical for charged lepton and missing p_T signatures of the decaying Ws and Zs. Other systematic errors like luminosity uncertainties, jet reconstruction efficiencies, or knowledge of the fractional contributions from WBF and QCD production are also eliminated by obtaining the background normalization from the leptonic $W,\ Z$ data. Even trigger efficiencies can be determined directly from these events.

The background normalization error can be further reduced by expanding the calibration region, at the price, however, of introducing a QCD uncertainty, due to the necessary extrapolation to the signal region. For the Zjj background in particular, one would like to use the

entire ϕ_{jj} region to determine the background normalization, since the data sample within (4) will be relatively small. These extrapolation uncertainties are small, as we will now show for the shape of the ϕ_{jj} distribution.

At present we only have leading order (LO) calculations of the Wjj and Zjj QCD backgrounds available. Due to the small difference in weak boson mass, as compared to *e.g.* the large dijet mass required in our event selection, QCD corrections for these processes are expected to be very similar and we only analyze the shape of the ϕ_{jj} distribution for the QCD Zjj background in the following. Shown in Fig. 4(a) is $d\sigma/d\phi_{jj}$ for four different renormalization scale choices, $\mu_R^0 = \sqrt{\hat{s}/4}$ (dash-dotted line) where $\hat{s}$ is the squared parton center–of–mass energy, $\mu_R^0 = \sqrt{(E_T^2(Z) + p_{Tj_1}^2 + p_{Tj_2}^2)/3}$ (dashed line), the default choice $\alpha_s^2(\mu_R^0) = \alpha_s(p_{Tj_1})\alpha_s(p_{Tj_2})$ (solid line), and $\mu_R^0 = E_T(Z)$ (dotted curve). One finds that the normalization of the QCD background changes by up to a factor of 3 between these choices and another variation by a factor of 3 to 4 is obtained by changing individual renormalization scales between $\mu_R = \mu_R^0/10$ and $\mu_R = 10\mu_R^0$. While the normalization of the QCD Zjj cross section changes drastically, the shape of the ϕ_{jj} distribution is essentially unaffected. As a measure of shape changes we plot the fraction of events with $\phi_{jj} < 1$,

$$R_1 = \frac{\int_0^1 \frac{d\sigma}{d\phi_{jj}}\, d\phi_{jj}}{\int_0^\pi \frac{d\sigma}{d\phi_{jj}}\, d\phi_{jj}}\ , \tag{5}$$

as a function of ξ, the scale factor for the four different renormalization scale choices $\mu_R = \xi\mu_R^0$ listed above. The ξ dependence shown in Fig. 4(b) is very small for individual choices of μ_R^0, smaller in fact, than the differences between the four basic scales μ_R^0.

Fig. 4(b) indicates that $R_1 = 0.19 \pm 0.02$ at LO QCD, i.e. a scale uncertainty of at most 10% is found for the shape of the ϕ_{jj} distribution, a very small QCD error indeed for a leading order calculation. While this error is still uncomfortably large for the actual determination of an invisible Higgs contribution to $jj\not{p}_T$ events, a NLO calculation, which hopefully will be available by the time the experiment is performed, should push the QCD shape uncertainty to well below the 5% level. We assume a 5% QCD uncertainty on R_1 in the following.

Compared to this extrapolation from opposite side to same side dijet events, minimal changes in hadronic event properties are encountered when extrapolating from Vjj events with observed leptons, as discussed above, to the corresponding $jj\not{p}_T$ sample. Hence QCD uncertainties for ratios like $\sigma(Zjj, Z \to \nu\bar{\nu})/\sigma(Zjj, Z \to l^+l^-)$, within analog cuts, are expected to be small. Indeed, an analysis of the scale uncertainties of these ratios, analogous to the one performed above for R_1, points to LO QCD errors of 3% or less for the Wjj ratios and 1-2% for the Zjj ratios. At NLO these QCD uncertainties should be entirely negligible and we do not consider them in the following.

V. DISCUSSION

The previous discussion points to at least two methods for constraining, or discovering, an invisible Higgs decay channel. The first uses the shape of the ϕ_{jj} distribution only. With 10 fb^{-1} already, the estimated 1670 background events in the $\phi_{jj} < 1$ region imply that R_1 in (5) can be measured with a statistical error of 2.2%, which is already small compared to

the systematic error of 5% due to QCD scale uncertainties. Taking the expectations for an $M_H = 120$ GeV Higgs boson as an example (see Table III), an invisible effective branching fraction $B_H = \mathrm{Br}(H \to \mathrm{invisible})$ would give rise to a modification

$$R_1 = \frac{1670 + 967 B_H}{9180 + 2380 B_H} = 0.182(1 + 0.32 B_H + \dots) \; . \tag{6}$$

In absence of a signal, a deviation of R_1 of more than 10.7% can be ruled out at 95% CL, which translates into an upper bound

$$B_H < 34\% \qquad \text{at 95\% CL} \; , \tag{7}$$

from shape information alone. Clearly this bound is systematics dominated and can be improved if it can be shown that our estimate for the QCD scale uncertainty is too conservative.

A much higher sensitivity is achieved by making use of charged lepton signatures for Vjj events, as discussed in the previous section. Again assuming an integrated luminosity of 10 fb^{-1}, the Wjj background can directly be determined from $W \to l\nu$ events in the region $\phi_{jj} < 1$, with a statistical error of 2.3%. The number of Zjj events with $Z \to l^+l^-$, in this region, is still modest, which makes it worthwhile to combine the direct determination with an extrapolation of the $(Z \to l^+l^-)jj$ cross section in the $\phi_{jj} > 1$ region, in spite of the 5% systematic uncertainty of R_1. Combining all errors in quadrature, the $(Z \to \nu\bar{\nu})jj$ background in $\phi_{jj} < 1$ can be predicted, directly from the data, with a 5.3% error. The combined background from Wjj and Zjj sources can thus be predicted with an accuracy of 3.0%. Combined with the expected statistical uncertainty of the 1670 background events, one finds that the Higgs contribution can be measured with a 1σ error of 6.4 fb, which, in absence of a signal, translates into a 95% CL bound of

$$B\sigma(qq \to qqH, \; H \to \mathrm{invisible}) < 12.5 \text{ fb}. \tag{8}$$

For an integrated luminosity of 100 fb^{-1} the combined backgrounds can be obtained with a precision of 1.2% and the bound (8) reduces to 4.8 fb. We present in Table IV the invisible Higgs branching ratio that can be probed at 95% CL as a function of M_H. In the event that the invisible Higgs production cross section is suppressed with respect to the SM, the limits in this table apply to the product of the invisible branching ratio times the suppression factor. We find that the WBF channel extends considerably the sensitivity for invisibly decaying Higgs bosons, with respect to the ZH and $\bar{t}tH$ channels [8,9]. With 10 fb^{-1} (100 fb^{-1}) of data it is possible to discover these particles with masses up to 480 GeV (770 GeV), at the 5σ level, provided their invisible branching ratio is 1.

A disadvantage of the WBF process, as compared to ZH and $\bar{t}tH$ production, is the requirement of a more complicated trigger. The latter provide hard isolated leptons as effective trigger signatures while the WBF signal possesses a dijet and missing p_T signature only. The two jets of the WBF signal are very hard and widely separated, however, which allows for the setup of a specific WBF trigger, with modest reliance on the Higgs decay signature. The QCD dijet cross section for events with two jets of $p_T > 40\ (20)$ GeV within $|\eta_j| < 5$, separated by $|\eta_{j_1} - \eta_{j_2}| > 4.4$, is about 2.3 (41) μb. Requiring the presence of $\not{p}_T$ with more than 3 to 4σ significance, a condition which is easily fulfilled by the signal events with their $\not{p}_T > 100$ GeV, will immediately lower these cross sections to the low nb level, *i.e.* to event rates of a few Hz

only at a luminosity of 10^{33}cm^{-2}sec^{-1}. Similarly, the presence of isolated electrons, muons or photons, of modest p_T, will allow for efficient triggers of $H \to \tau\tau$, $H \to WW$ and $H \to \gamma\gamma$ events in WBF [10–12]. We strongly urge the LHC detector collaborations to develop such triggers for a broad-based study of WBF processes.

ACKNOWLEDGMENTS

D. Z. would like to thank the CERN theory group for its hospitality during the early stages of this work. Enlightening discussions with S. Dasu, A. Nikitenko, and D. Rainwater are gratefully acknowledged. This work was supported in part by the University of Wisconsin Research Committee with funds granted by the Wisconsin Alumni Research Foundation, in part by the U. S. Department of Energy under Contract No. DE-FG02-95ER40896, by Conselho Nacional de Desenvolvimento Científico e Tecnológico (CNPq), by Fundação de Amparo à Pesquisa do Estado de São Paulo (FAPESP), and by Programa de Apoio a Núcleos de Excelência (PRONEX).

REFERENCES

[1] H. Haber, D. Dicus, M. Drees, and X. Tata, Phys. Rev. **D37**, 1367 (1987); J. F. Gunion and H. E. Haber, Nucl. Phys. **B307**, 445 (1988); K. Griest and H. E. Haber, Phys. Rev. **D37**, 719 (1988); A. Djouadi, *et al.*, Phys. Lett. **B376**, 220 (1996); A. Djouadi and M. Drees, Phys. Lett. **B407**, 243 (1997).

[2] R. E. Shrock and M. Suzuki, Phys. Lett. **B10**, 250 (1982); L. F. Li, Y. Liu, and L. Wolfenstein, Phys. Lett. **B159**, 45 (1985).

[3] A. S. Joshipura and J. W. F. Valle, Nucl. Phys. **B397**, 105 (1993).

[4] N. Arkani-Hamed, S. Dimopolous, and G. Dvali, Phys. Lett. **B429**, 263 (1998).

[5] G. F. Giudice, R. Rattazzi, and J. D. Wells, hep-ph/0002178.

[6] P. Janot, "Testing the neutral Higgs sector of the MSSM with a 300–500 GeV e^+e^- collider", report LAL 91-61 (1991) and DESY 92-123A (1992) 107; O. J. P. Éboli *et al*, Nucl. Phys. **B421**, 65 (1994); A. Djouadi, Int. J. Mod. Phys. **A10**, 1 (1995); F. de Campos *et al*, Phys. Rev. **D55**, 1316 (1997).

[7] ALEPH Collaboration (R. Barate *et al.*), Phys. Lett. **B466**, 50 (1999); DELPHI Collaboration (P. Abreu *et al.*), Phys. Lett. **B459**, 367 (1999); L3 Collaboration (M. Acciarri *et al.*), Phys. Lett. **B485**, 85 (2000); P. I. Kemenes, talk given at the XXXth International Conference on High Energy Physics, Osaka 2000 (http://ichep2000.hep.sci.osaka-u.ac.jp/scan/0801/pl/igokemenes/index.html).

[8] Debajyoti Choudhury and D. P. Roy, Phys. Lett. **B322**, 368 (1994).

[9] J. F. Gunion, Phys. Rev. Lett. **72**, 199 (1994).

[10] D. Rainwater and D. Zeppenfeld, JHEP **971**, 005 (1997).

[11] D. Rainwater and D. Zeppenfeld, Phys. Rev. **D60**, 113004 (1999), erratum-*ibid.* **D61**, 099901 (2000).

[12] D. Rainwater, D. Zeppenfeld, and K. Hagiwara, Phys. Rev. **D59**, 014037 (1999).

[13] V. Barger, T. Han, J. Ohnemus, and D. Zeppenfeld Phys. Rev. Lett. **62**, 1971 (1989); Phys. Rev. **D40**, 2888 (1989).

[14] H. Chehime and D. Zeppenfeld, Phys. Rev. **D47**, 3898 (1993); D. Rainwater, R. Szalapski, and D. Zeppenfeld, Phys. Rev. **D54**, 6680 (1996).

[15] T. Stelzer and W. F. Long, Comput. Phys. Commun. **81**, 357 (1994).

[16] H. L. Lai *et al.*, Phys. Rev. **D55**, 1280 (1997).

[17] V. Barger, R. J. N. Phillips, and D. Zeppenfeld, Phys. Lett. **B346**, 106 (1995).

[18] D. Rainwater, PhD thesis, report hep-ph/9908378.

	signal Hjj	QCD Zjj and Wjj	EW Zjj and Wjj
P_{surv}	0.87	0.28	0.82

TABLE I. Survival probabilities for the signal and background for a veto of central jets with $p_T > 20$ GeV. From Ref. [18].

	QCD Zjj	QCD Wjj	EW Zjj	EW Wjj	total
σ	1254	1284	151	101	2790
$P_{surv}\ \sigma$	351	360	124	83	918
$P_{surv}\ \sigma(\phi_{jj} < 1)$	71.8	70.2	14.8	9.9	167

TABLE II. Total cross sections (in fb) for the backgrounds after applying the cuts (1-3) (first two lines) and (4). In the last two lines we also include the central jet veto survival probabilities of Table I.

M_H (GeV)	110	120	130	150	200	300	400
σ	282.	274.	266.	251.	214.	154.	110.
$P_{surv}\ \sigma$	245.	238.	232.	218.	186.	134.	95.7
$P_{surv}\ \sigma(\phi_{jj} < 1)$	99.4	96.7	94.3	89.2	77.0	56.3	40.7

TABLE III. Same as Table II for the signal at several invisible Higgs masses, assuming Br($H \to$ invisible$) = 1$. Cross sections are given in fb.

M_H (GeV)	110	120	130	150	200	300	400
10 fb^{-1}	12.6%	13.0%	13.3%	14.1%	16.3%	22.3%	30.8%
100 fb^{-1}	4.8%	4.9%	5.1%	5.3%	6.2%	8.5%	11.7%

TABLE IV. Invisible branching ratio that can be probed at 95% CL as a function of M_H for an integrated luminosity of 10 fb^{-1} and 100 fb^{-1}. A SM production cross section is assumed.

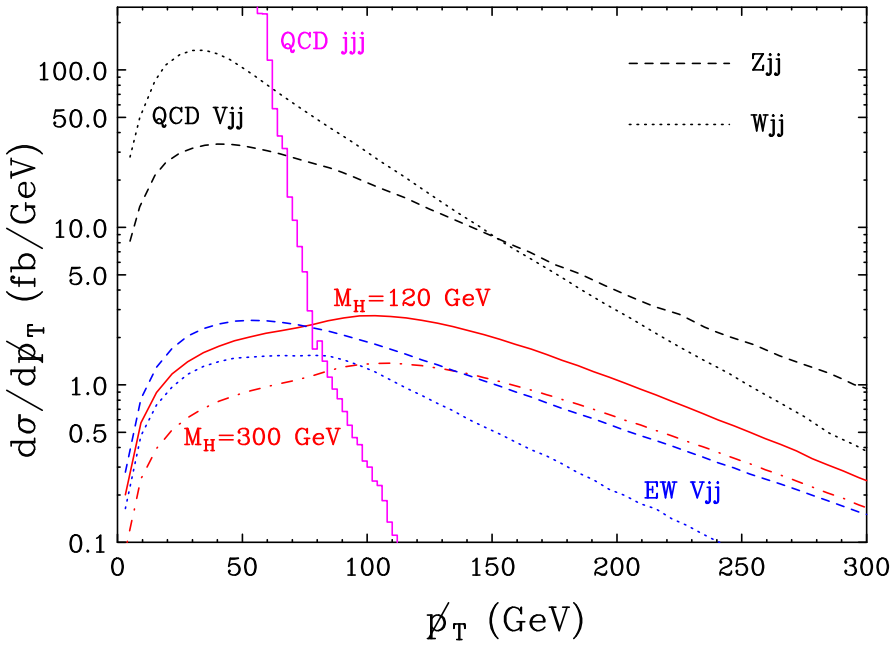

FIG. 1. Missing transverse momentum spectra within the cuts (1) and (3). Results are shown separately for the EW Zjj (blue dashed line) and Wjj (blue dotted line) backgrounds, as well as the QCD processes Zjj (black dashed line), Wjj (black dotted line), and jjj (magenta histogram) production. We exhibit the invisible Higgs contribution for $M_H = 120$ (red solid line) and 300 GeV (red dot-dashed line).

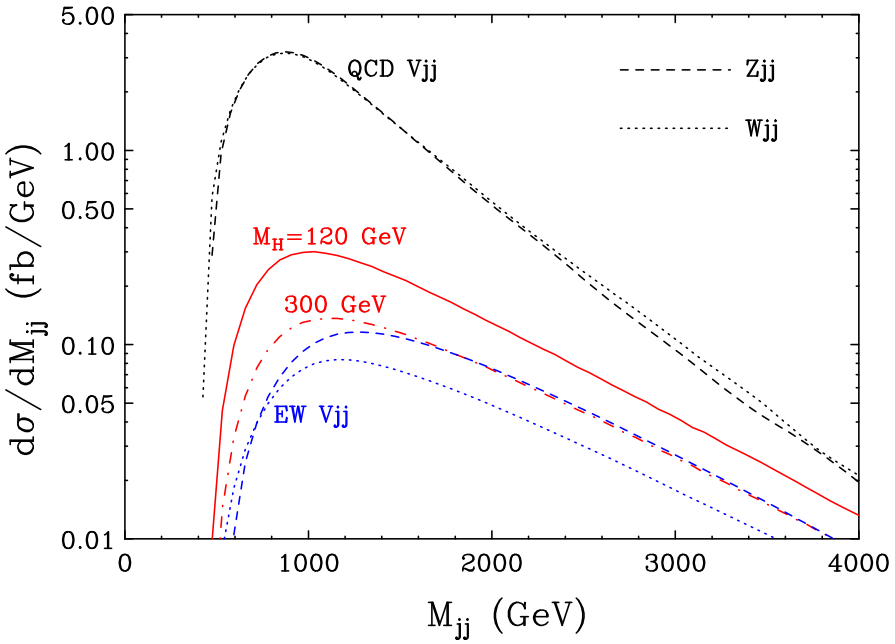

FIG. 2. Dijet invariant mass distributions when applying the cuts of Eqs. (1,2). The lines follow the same convention as in Fig. 1.

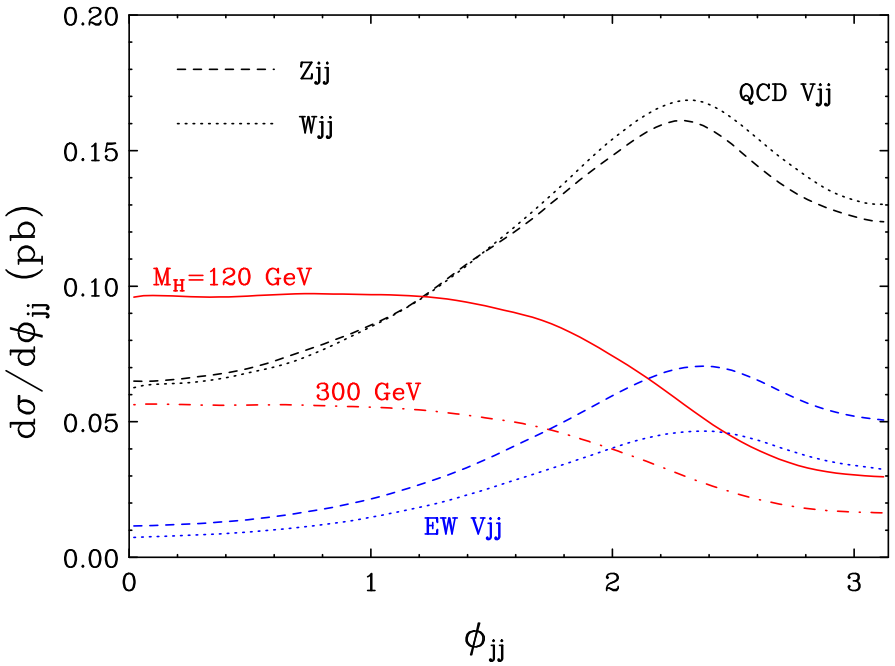

FIG. 3. Distributions of the azimuthal angle separation between the two tagging jets for the various background processes and the Higgs signal at $M_H = 120$ and 300 GeV. Results are shown after applying the cuts (1-3) and including the effect of a central jet veto with the survival probabilities of Table I. The lines follow the same convention as in Fig. 1.

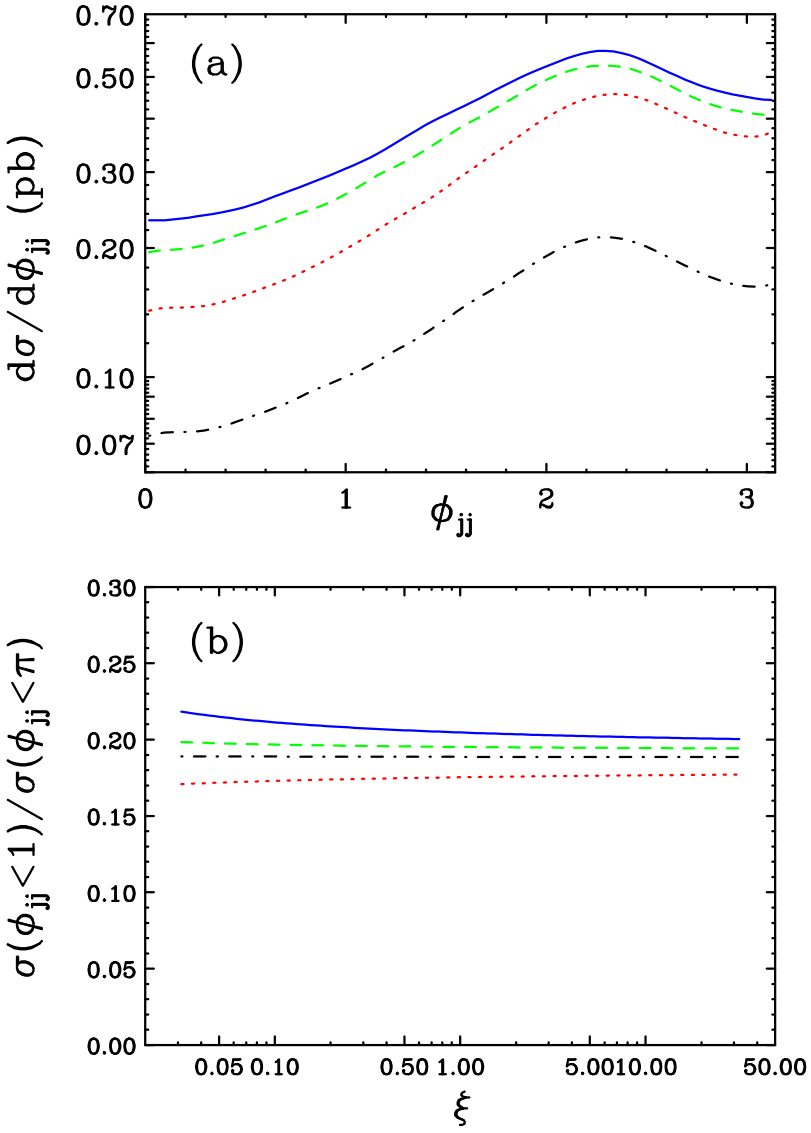

FIG. 4. Scale dependence of the shape of the dijet azimuthal angle distribution of QCD Zjj events with $Z \to \nu\bar{\nu}$ in LO QCD. Results are shown for four choices of the basic renormalization scale, $\mu_R^0 = \sqrt{\hat{s}/4}$ (dash-dotted line), $\mu_R^0 = \sqrt{(E_T^2(Z) + p_{Tj_1}^2 + p_{Tj_2}^2)/3}$ (green dashed line), the default choice $\alpha_s^2(\mu_R^0) = \alpha_s(p_{Tj_1})\ \alpha_s(p_{Tj_2})$ (blue solid line), and $\mu_R^0 = E_T(Z)$ (red dotted curve). In (b) the fraction of events with $\phi_{jj} < 1$ is shown as a function of ξ, where $\mu_R = \xi\mu_R^0$.